2014 International Joint Conference on Neural Networks (IJCNN)
July 6-11, 2014, Beijing, China

Alzheimer's Disease Classification Based on Gait Information

Wei-Hsin Wang, Yu-Liang Hsu, Ming-Chyi Pai, Cheng-Hsiung Wang, Chun-Yao Wang, Chien-Wen Lin, Hao-Li Wu, and Pau-Choo Chung

***Abstract*—Alzheimer's disease (AD) is becoming one of the major diseases of the elderly. Traditionally, patients take questionnaires or do some balance tests for clinical evaluation. However, results with such evaluation are subjective. For more objective quantitative measurement, this paper uses an inertial-sensor-based device to measure the gait information while participants walking. In the experiment, the participants are asked to walk on a 40m strike line and take single-task and dual-task tests. In the dual-task test, the participants are asked to count down from 100. This paper presents a stride detection algorithm to automatically acquire gait information of each gait cycle from the acceleration and angular velocity signals. Features are calculated from those inertial signals. After feature generation, we do feature selection to select the significant feature. Then, a probabilistic neural networks (PNNs) is used to classify if the participants suffer from AD. In this paper, we provide an objective way to evaluate the situation of the participants. The experimental results successfully validate the effectiveness of the proposed device and the proposed algorithm with an overall classification accuracy rates are 63.33% and 70.00% in women and men group, respectively.**

I. INTRODUCTION

THE rapidly increasing number of the elderly has widespread effect to our public health system. The health care and aging-associated services face with the problem of shortage of resources. The number of older people over 60 years will double from about 11% to 22% between 2000 and 2050. Meanwhile, the number of older people aged 60 years and over is expected to become 2 billion from 605 million [1]. One of the most important diseases relative to age is Alzheimer's disease (AD). Many researches showed that AD is an age-associated neurodegenerative disease [2-6]. With the increase in the elderly population, the number of AD patients will grow. Unfortunately, the growing population of AD patients has become a serious problem and results in a heavy social burden [7]. In 2006, 26.6 million people were afflicted by AD, and the number would quadruple by 2050 [8].

How to detect the disease earlier and have proper treatment is very important. The cognitive function of neuropsychological can be used to assist clinical diagnosis. Mini-Mental State Examination (MMSE) and Cognitive Assessment Screening Instrument (CASI) are two common neuropsychological tests to evaluate the cognitive dysfunction and memory impairment.

Pau-Choo Chung is with the Department of Electrical Engineering, National Cheng-Kung University, Tainan, Taiwan 701 ROC (phone: 886-6-2757575 ext. 62373; fax: 886-6-2345482; e-mail: pcchung@ee.ncku.edu.tw).

This work was supported by the National Science Council of the Republic of China, Taiwan, under a Sino-Franco jointed project with grant: NSC99-2923-E-006-001-MY3.

Balance ability and gait abnormalities are also the indicators for cognitive function and AD evaluation. Common assessment methods are Berg Balance Scale (BBS), Time-Up and Go Test (TUGT), and Short Physical Performance Battery (SPPB). Berg Balance Scale [9] has 14 daily life movements for elderly people's static and dynamic balance ability evaluation. Time-Up and Go Test [10] is a test for the functional mobility assessment. In the test, subjects need to stand up from an arm chair first, then walk 3 meters, turns, walk back and sit down on the arm chair. The SPPB test [11] asks subjects to have various standing ways for balance evaluation, including standing with the feet together in the side-by-side, semi-tandem, and tandem positions.

Pettersson *et al.* [12] used BBS, TUGT, Frenchay Activities Index (FAI), and "figure 8" walk to estimate the balance ability of the elderly with healthy elderly and elderly with mild AD. Pettersson *et al.* [13] also used the BBS, TUGT, FAI, TUG manual (diffTUGT), Talking While Walking (TWW), and Tinetti balance tests to evaluate the activity level and motor function of the subjects, who had no cognition impairment, mild cognition impairment (MCI), AD, and other dementia. The result showed that the motor function was affected in very mild AD. The MCI subjects and the AD subjects had difficulties to perform a cognitive task while walking. Romdhane *et al.* [14] used the SPPB to obtain the gait and walking parameters in activities for the assessment of AD symptoms. The result indicated that the AD subjects presented an obvious shorter stride length and slower stride speed.

However, based on the above literature survey, the assessments need to be recorded manually and might cause measurement deviation. To be more accurate, some instruments were developed to record the information while the patients were doing examines. For example, Nadkarni *et al.* [15] compared gait parameters between early AD patients and health control group by using footswitches. The results show that the AD patients have slower velocity, slower cadence and shorter stride length than HCs. Nakamura *et al.* [16] videotape ten consecutive walking patterns of the patients to study the relationship between falls and stride length variability in senile dementia of the Alzheimer type (SDAT). Webster *et al.* [17] used the GAITRite walkway system® (CIR Systems, Inc., 60 Garlor Drive Havertown, PA 19083) to record subjects' spatial and temporal gait information. The system is an electronic mat consisting of pressure-activated sensors arranged in grid formation. Gillain *et al.* [18] combined the electrical photocells and the Locometrix® triaxial accelerometer to measure walking speed, stride frequency, stride length, symmetry, and

978-1-4799-1484-5/14/$31.00 ©2014 IEEE

regularity in elderly people with MCI and AD patients.

In this paper we develop inertial sensors. The sensors are worn on the feet and to collect the signals while the patients are walking. The signals are used to develop an algorithm for clinical diagnosis of Alzheimer's disease assistance. Those signals are preprocessed by the calibration and low-pass filter. After signal preprocessing, 11 features are extracted from each axis in the accelerations and angular velocities. To get better classification result and to reduce computational load, feature selection is used to select a subset of significant features. After feature selection, we use the probabilistic neural networks (PNNs) to know if the participants suffer from AD. The result shows that the recognition rate is 63.33% and 70.00% in the women and men group, respectively.

The remainder of this paper is organized as follows. In Section II, we introduce the hardware components of the wearable inertial sensor system in detail. The proposed classification scheme, including the stride detection, is discussed in Section III. In Section IV, experimental results are presented and the conclusion is provided in the final section.

II. Wearable Inertial Sensor Module

A wearable inertial sensor module is developed to sense and record gait motion accelerations and angular velocities. The wearable inertial sensor module consists of a triaxial accelerometer (ADXL345), a uniaxial gyroscope (LY530ALH), a biaxial gyroscope (LPR530AL), a microcontroller (STM32F103), and a micro SD flash memory card. The accelerations detected by the accelerometer and the angular velocities detected by the gyroscopes are processed by the microcontroller and saved into the memory card. The sensitivity of the accelerometer is set from -4g to +4g and the gyroscopes are set the full-scale range and sensitivity to ±300 °/s and 3.33 mv/°/s, respectively. All of the signals are sampled at 100 Hz. The dimensions of the inertial sensor module are 45 mm × 32 mm × 8 mm as shown in Fig. 1.

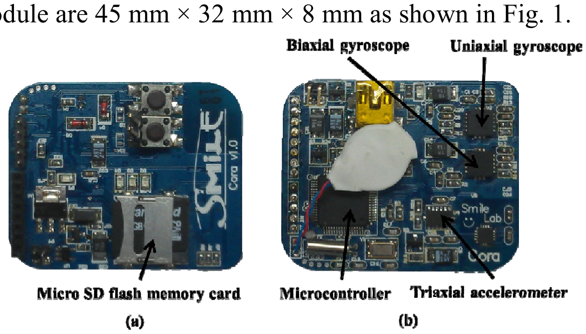

Fig. 1. Inertial-sensor-based wearable hardware device. (a) Front view of the circuit. (b) Back view of the circuit.

III. Automatic Cognitive Assessment and Classification Scheme

An automatic cognitive assessment and classification scheme is developed to perform the cognitive assessment for patients with Alzheimer's disease (AD) and to classify whether the participant is an AD patient by using the signals measured by the accelerometer and gyroscopes embedded in the wearable inertial sensor module. The procedures of the proposed automatic cognitive assessment and classification scheme composed of 1) signal preprocessing; 2) stride detection; 3) feature extraction; 4) feature normalization; 5) feature selection; 6) cognitive assessment; and 7) classifier construction. As the dynamic intervals of the strides during the walking tasks are obtained through the stride detection algorithm, the features are extracted from the filtered acceleration and angular velocity signals within each dynamic interval of each stride. All extracted features are normalized to avoid the effects of the value ranges from different parameters via the feature normalization subsequently. Moreover, the feature selection is used to obtain characteristic features to reduce the computational complexity and improve classification rates. Finally, we use the linear-regression model and the probabilistic neural network (PNN) classifier to assess the cognitive function and to classify whether the participant is an AD patient. The procedure of the proposed automatic cognitive assessment and classification scheme is shown in Fig. 2.

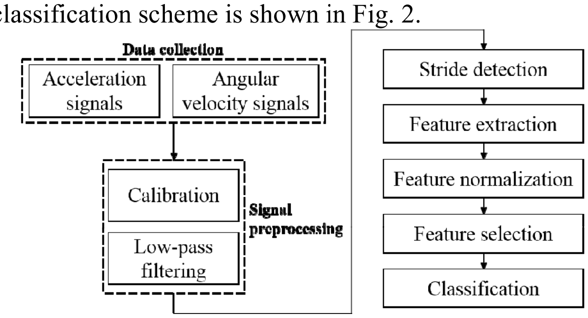

Fig. 2. Procedure of the proposed automatic cognitive assessment and classification scheme.

A. Signal Preprocessing

The high-frequency noise and hardware deviation might cause error; therefore, the signal preprocessing is used to reduce the problem. In this paper, the signal preprocessing consists of the hardware calibration and signal low-pass filter.

a) Calibration of Inertial Sensors

Non-unit scale factor and the non-zero bias are two factors in the hardware deviation. These two factors, which are associated with conformation and material, play an important role of calibrating inertial sensors. The scale factor denotes the ratio of the measured output to the sensor input and the bias represents the offset error. The output of the accelerometer contains only gravity when it is stationary. Hence, the triaxial accelerometer is placed on a horizontal surface first and each axis is aligned with gravity in the same and opposite direction alternatively. We can use the following equations to obtain the scale factor (SF_{acc}) and the bias (B_{acc}) of the accelerometer and then to acquire the calibrated measurements (A_c) in each axis of the triaxial accelerometer:

$$SF_{acc} = \frac{2g}{V(+g) - V(-g)}, \tag{1}$$

$$B_{acc} = \frac{V(+g) + V(-g)}{V(+g) - V(-g)} \times g, \tag{2}$$

$$A_c = SF_{acc} \times V_{acc} + B_{acc}, \tag{3}$$

where $V(+g)$ and $V(-g)$ are the voltage outputs in each axis of the accelerometer when it is aligned with the same direction of gravity and with the opposite direction of gravity, respectively. SF_{acc} is in g per volts (g/V) while B_{acc} is in g, where g is the gravitational acceleration. V_{acc} is the output voltage in each axis of the accelerometer.

To calibrate gyroscopes, the equation (4), which is similar to (3), is used. Nevertheless, the scale factor (SF_{gyro}) (°/s/V) in each axis of the gyroscopes can be obtained from the datasheet. In ideal situation, the output of each axis of the gyroscopes should be zero when the device is stationary. Therefore, the bias (B_{gyro}) (°/s) of each axis of the gyroscope is calculated as the mean of the angular velocity in each axis. The calibration equation of the gyroscope is as follows:

$$W_c = SF_{gyro} \times V_{gyro} + B_{gyro}, \tag{4}$$

where W_c is the calibrated angular velocity and is in °/s. V_{gyro} is the output voltage in each axis of the gyroscopes.

b) Low-pass Filter

In this paper, a moving average filter is used to reduce the high-frequency noise. The filter is expressed as follow:

$$y[n] = \frac{1}{N} \sum_{i=1}^{N} x[n-i], \tag{5}$$

where $x[n]$ is the calibrated data and $y[n]$ is the filtered data. The N is the number of points, we select $N = 10$ in the moving average in this study.

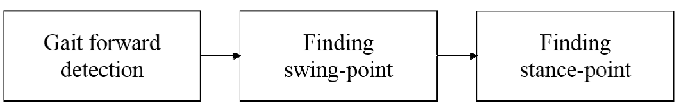

Fig. 3. The procedure of the stride detection algorithm

B. Stride Detection

In this paper, a stride detection algorithm is developed to automatically acquire gait information of each gait cycle from the filtered acceleration and angular velocity signals. Those signals are generated from walking motions during the single-task and dual-task walking. The proposed stride detection algorithm based on a threshold method is composed of 1) gait forward detection; 2) finding swing-point; and 3) finding stance-point. The procedure of the stride detection algorithm is shown in Fig. 3. The steps of the proposed stride detection algorithm are illustrated as follows.

Step 1 Detecting gait forward: Because of the way we wear the device, the y-axis of gyroscope can present the rotation of the foot while walking. Then we use the y-axis of gyroscope signal to detect the forward motion. First, we find the peaks

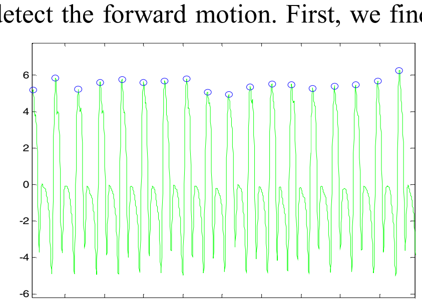

Fig. 4. The peak detected from the angular velocity signal. swing-points.

on the signal, and then we set a threshold. A real forward motion of a stride is considered when the peak is higher than the threshold. The result is shown in Fig. 4.

Step 2 Finding swing-point: The swing-points, which mean the time to start a forward motion, are found before the peaks are detected from Step 1. As we know, the swing-point must have an inverse angular velocity signal that causes a local minimum. We therefore find the first local minimum before each peak. That is considered as the swing-point.

Step 3 Finding stance-point: The stance-points, which mean the end of a forward motion, are found after the peaks are detected from Step 1. The stance-point, as the swing-point, has an inverse angular velocity signal that causes a local minimum. And we thus find the first local minimum after each peak, which is considered as the stance-point.

Fig. 5 shows the result after the stride detection algorithm. Once the swing-points and stance-points are determined, we calculate gate features.

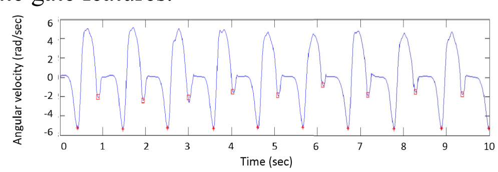

Fig. 5. The y-axis angular velocity signal of the gyroscope. Star shape: swing-points. Square shape: stance-points.

C. Feature Extraction

Once the 20 dynamic intervals of each subject during each walking task are obtained, the features of each dynamic interval of each stride can be extracted from the filtered x-, y-, and z-axis accelerations and angular velocities generated from the walking motions. The quantitative gait features, including 1) mean, 2) standard deviation, 3) variance, 4) interquartile range, 5) mean absolute deviation, 6) root mean square, 7) skewness, 8) kurtosis, 9) energy, 10) gait symmetry, and 11) gait regularity, are introduced as follows. And the total 66 (= 2 × 3 × 11) features are summarized in Table I.

1) Mean: The mean value of the acceleration and angular velocity signals is the dc component of the signals in each dynamic interval.

$$Mean = \bar{x} = \frac{1}{N} \sum_{i=1}^{N} x_i. \tag{8}$$

2) Standard deviation (SD): The standard deviation is the square root of the variance.

$$SD = \sqrt{\frac{\sum_{i=1}^{N}(x_i - \bar{x})^2}{N-1}}. \tag{9}$$

3) Variance (VAR): The variance value of the acceleration and angular velocity signals are calculated as follows:

$$VAR = \frac{\sum_{i=1}^{N}(x_i - \bar{x})^2}{N-1}, \tag{10}$$

where x_i is the acceleration or angular velocity signals, $\bar{x}$ is the mean value of x_i, and N is the data number in each dynamic interval in (8)-(10).

4) Interquartile range (IQR): IQR is the difference between the 75th percentile value and the 25th percentiles value.

5) Mean absolute deviation (MAD):

$$MAD = \frac{\sum_{i=1}^{N}|x_i - \bar{x}|}{N}. \tag{11}$$

6) Root mean square (RMS):

$$RMS = \sqrt{\frac{\sum_{i=1}^{N} {x_i}^2}{N}}. \tag{12}$$

7) Skewness: Skewness is the symmetry of the acceleration and angular velocity signals.

$$skewness = \frac{E(x-\bar{x})^3}{\sigma^3}. \tag{13}$$

8) Kurtosis: Kurtosis is to measure whether the acceleration or angular velocity signals are peaked or flat relative to a normal distribution.

$$kurtosis = \frac{E(x-\bar{x})^4}{\sigma^4}, \tag{14}$$

where $E(.\ )$ is the expected value, $\bar{x}$ is the mean value of the acceleration or angular velocity signals, and σ is the standard deviation of the acceleration or angular velocity signals in (13) and (14).

9) Energy: Energy is calculated as the sum of the magnitudes of squared discrete fast Fourier transform (FFT) components of the signals.

$$Energy = \frac{\sum_{i=1}^{n}|f_i|^2}{n}, \tag{15}$$

where f_i is the i^{th} FFT component of the acceleration or angular velocity signals. $|f_i|$ is the magnitude of f_i.

10) Gait symmetry: Calculate the cross-correlation between right foot's interpolated data and left foot's interpolated data in the same gait cycle. In this paper, we interpolated the acceleration and angular velocity signals in each gait segment to 200 data points.

$$CC_{symmetry} = \sum_{n=1}^{N} x_{r(n)}^{i} x_{l(n)}^{i}\ , \tag{16}$$

where N is total number of points in gait, $x_{r(n)}^{i}$ is the accerleration or angular velocity signals of the n^{th} data point in i^{th} gait cycle from right foot, $a_{l(n)}^{i}$ is the accerleration or angular velocity signals of the n^{th} data point in i^{th} gait cycle from left foot.

11) Gait regularity: Calculate the cross-correlation between one and the following gait.

$$CC_{regularity} = \sum_{n=1}^{N} x_{r(n)}^{i} x_{r(n)}^{i+1}\ , \tag{17}$$

where N is the total number of data points in gait, $x_{r(n)}^{i}$ is the accerleration or angular velocity signals of the nth data point in ith gait cylce from right foot, $x_{r(n)}^{i+1}$ is the accerleration or angular velocity signals of the nth data point in the following gait cycle from right foot.

TABLE I
GAIT FEATURES USED IN THIS STUDY

Signal type	Axis	Feature name
Acceleration signals	x- y- z-	1) Mean
		2) SD
		3) VAR
		4) IQR
		5) MAD
		6) RMS
		7) Skewness
Angular velocity signals		8) Kurtosis
		9) Energy
		10) $CC_{symmetry}$
		11) $CC_{regularity}$

D. Feature Normalization

The difference of the value ranges of the abovementioned 66 features may influence the performance of the classification. In order to eliminate the effects of the ranges, we normalize each feature individually by using z-score. The equation of the normalization is shown as follows.

$$y = \frac{x-\mu}{\sigma}, \tag{18}$$

where x and y are the original value and normalized value of each feature, respectively. μ is the mean of the original values and the σ is the standard deviation of the original values.

E. Feature Selection

A feature selection method is employed to select a subset of significant features for reducing computational load and improving classification accuracy. A representative feature selection method is utilized in this paper: the sequential forward selection (SFS) which is a bottom-up feature selection. Suppose that we want to choose an m-dimensions feature subset from original feature set. SFS starts from the empty feature set, sequentially add one feature from original feature set which results in the best classification rate. Finally, we can obtain an optimal m-dimensions feature subset.

F. Classifier Construction

In this paper, we use the probabilistic neural networks (PNNs) to differentiate the participants with and without AD via the gait features. The PNN proposed by Specht is based on Bayes' strategy and designed for dealing with classification problems. The PNN is composed of four layers including an input layer, a pattern layer, a summation layer, and an output layer. Fig. 6 shows the structure of the PNN. Now, we introduce the training and testing stages in detail, respectively.

Training Stage: Training sample $\mathbf{X} = \{X_1, X_2, \cdots, X_N\}$ is used to train the PNN, where N is the number of the training sample. Each sample includes a selected feature subset $\mathbf{X}_j = \mathbf{S}^j = [s_1^{(j)}, s_2^{(j)}, \ldots, s_n^{(j)}]^{\mathrm{T}}$ with n dimensions, which is extracted from j^{th} dynamic interval of j^{th} stride and can be taken as the training input features of the network, where $j \in \{1, 2, \cdots, N\}$. The number of the neurons in the input and pattern layers are equal to n and N, respectively. The synaptic weight $w_{j,i}{}^{(P)}$ between the i^{th} neuron in the input layer and the j^{th} neuron in the pattern layer is defined as follows:

$$w_{j,i}^{(P)} = s_i^{(j)}. \tag{21}$$

This is, $w_{j,i}^{(P)}$ is immediately assigned the value of i^{th} feature extracted from j^{th} training sample, where $i \in \{1, 2, \cdots, n\}$. The number of neurons in the summation layer is equal to the number of the classes (N_c), which equals to 2 in this paper. The synaptic weight $w_{k,j}{}^{(S)}$ between the j^{th} neuron in the pattern layer and the k^{th} neuron in the summation layer is defined as follows:

$$w_{k,j}^{(S)} = \begin{cases} 1 & if\ X_j \in C_k, \\ 0 & otherwise, \end{cases} \tag{22}$$

where C_k means the k^{th} class. The value of $w_{k,j}{}^{(S)}$ is equal to 1 only when the input sample belongs to class k. The number of neurons in the competitive output layer equals to 1. The synaptic weight $w_{1,k}{}^{(O)}$ between the k^{th} neuron in the summation layer and the neuron in the output layer is defined as follows:

$$w_{1,k}^{(o)} = 1. \tag{23}$$

In general, the PNN is created with zero error by using the training sample.

Testing Stage: Once the PNN is trained, a testing sample $\bar{\mathbf{X}} = \bar{\mathbf{S}} = [\bar{s}_1, \bar{s}_2, \ldots, \bar{s}_n]^{\mathrm{T}}$ with n dimensions is used to test the trained PNN, which is taken as the testing input features of the network. The definitions and activation functions of each layer of the PNN used in this paper are described in the following.

1) Input layer: The input features $\{\bar{s}_1, \bar{s}_2, \ldots, \bar{s}_n\}$ are conveyed to the neurons in the pattern layer directly.

2) Pattern layer: The distance between the testing sample $\bar{\mathbf{S}} = [\bar{s}_1, \bar{s}_2, \ldots, \bar{s}_n]^{\mathrm{T}}$ and the training sample is calculated in this layer. The exponential activation function is described as follows:

$$P_j = \exp\left(-\frac{\sum_{i=1}^{n}(w_{j,i}^{(P)} - \bar{s}_i)^2}{2\sigma_j^2}\right), \tag{24}$$

where σ_j is the smoothing parameter.

3) Summation layer: The neurons in this layer calculate the maximum likelihood of the input sample $\bar{\mathbf{S}} = [\bar{s}_1, \bar{s}_2, \ldots, \bar{s}_n]^{\mathrm{T}}$ belonging to the class k. The output value of the k^{th} neuron in the summation layer is defined as S_k.

$$S_k = \frac{\sum_{j=1}^{N} w_{k,j}^{(S)} \times P_j}{\sum_{j=1}^{N} w_{k,j}^{(S)}}, \tag{25}$$

where P_j is the j^{th} neuron output in the pattern layer.

4) Summation layer: The neuron in this layer compares all the outputs of the summation layer and estimates the numerical label according to the maximum probability value.

$$C = \arg\max_{k \in \{1,2,\ldots,Nc\}} S_k, \tag{26}$$

where C denotes the estimated class of the testing sample $\bar{\mathbf{X}}$. In this paper, the output of the PNN is shown as the label of the two kinds of participants (i.e., healthy control and AD patients are labeled as ‘1’ and ‘2’, respectively.)

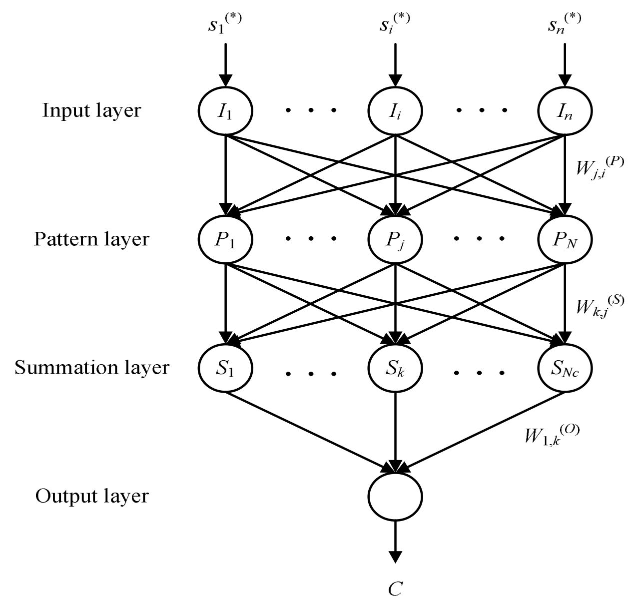

Fig. 6. Structure of PNN.

IV. Experimental Results

The effectiveness of the proposed algorithm of the physical activity classification is validated by using 10-fold, 5-fold, 2-fold, and LOSO (Leave one subject out). Acceleration signals are collected from 60 subjects. Participant demographic information and experimental results will be shown in Sections IV.A and IV.B.

A. Participants

In this paper, all of the participants are referred to the Department of Neurology at National Cheng Kung University Hospital, according to the professional diagnosis by Dr. Pai. Table II shows the demographics information in which the participants are divided into two groups: AD and HC. There are 30 participants (15 males and 15 females) in the AD group and 30 participants (15 males and 15 females) in the HC group. In the AD group, the mean age is 60.20 and 55.47 in men and women, respectively. In the HC group, the mean age is 63.40 and 64.80 in men and women, respectively. The Mini

Mental State Examination (MMSE) and Cognitive Assessment Screening Instrument (CASI) are two common neuropsychological tests, which we use to evaluate the cognitive dysfunction and memory impairment in all participants. The score range of MMSE is from 0 to 30, score lower than 24 is considered as memory impairment. The CASI score is from 0 to 100, score under 80 is considered as cognitive impairment. In this paper, the CASI scores in the HC group are 95.27±2.79 and 94.87±2.83 in men and women, respectively. And the scores in the AD group are 79.13±10.15 and 80.20±11.53 in men and women, respectively. On the other hand, the MMSE scores in the HC group are 28.40±1.59 and 28.40±1.24 in men and women, respectively. And the MMSE scores in the AD group are 22.40±3.38 and 23.73±3.65 in men and women, respectively.

TABLE II
DEMOGRAPHIC INFORMATION OF PARTICIPANTS

		HC	**AD**
Men	*n*	15	15
	Age, y	60.20±6.87	63.40±9.28
	Height, cm	167.97±7.41	164.77±7.95
	MMSE	28.40±1.59	22.40±3.38
	CASI	95.27±2.79	79.13±10.15
Women	*n*	15	15
	Age, y	55.47±5.11	64.80±5.03
	Height, cm	160.33±4.17	154.83±6.24
	MMSE	28.40±1.24	23.73±3.65
	CASI	94.87±2.83	80.20±11.53

B. Results

In this paper, we separate the group by gender because of the biological difference. In each group, we use feature selection to find out the significant features and the results are shown in Table III.

TABLE III
THE RESULTS OF FEATURE SELECTION

	Selected feature			
	Feature name	Axis	Signal	Test
Women	MAD	Y	Gyro	Single
	Regularity	Y	Gyro	Dual
	Regularity	Y	Acceleration	Dual
	Regularity	X	Acceleration	Dual
	IQR	X	Gyro	Single
	Skewness	X	Acceleration	Dual
	Kurtosis	X	Acceleration	Dual
	Kurtosis	Z	Gyro	Dual
	Symmetry	Y	Gyro	Single
Men	Kurtosis	X	Gyro	Dual
	Kurtosis	Y	Gyro	Dual
	IQR	Z	Gyro	Dual

After the feature selection, the PNN is used for the differentiation finding in the participants with and without AD. In this paper, we use 10-fold, 5-fold, 2-fold, and LOSO (Leave one subject out) to get the PNN results. The results are shown below in Table IV.

TABLE IV
THE RECOGNITION RATE, SENSITIVITY, AND SPECIFICITY IN THE WOMEN AND MEN GROUP

		Recognition rate (%)	Sensitivity	Specificity
Women	10-fold	56.67	0.67	0.47
	5-fold	63.33	0.65	0.68
	2-fold	60.00	0.50	0.75
	LOSO	63.33	0.67	0.60
Men	10-fold	70.00	0.69	0.72
	5-fold	66.67	0.65	0.65
	2-fold	70.00	0.62	0.81
	LOSO	70.00	0.67	0.73

V. CONCLUSION

An algorithm for the stride detection and classification by using inertial signals is presented in this paper. During the experiment, inertial signals are collected from the device we developed. The device is mounted on the participants' foot. The proposed stride detection algorithm is used to detect each stride and calculate the features from the signals. Consider the physiological difference between women and men, the participants are divided into two groups by gender. SFS is used to do feature selection in each group. After the feature selection, those features are tested by the PNN in 2-fold, 5-fold, 10-fold, and LOSO. The results show that the recognition rate is 63.33% and 70.00% in women and men group, respectively.

REFERENCES

[1] "Ageing and Life Course, WHO," *http://www.who.int/ageing/en/*, 2013.

[2] R. Brookmeyer, S. Gray, and C. Kawas, "Projections of Alzheimer's disease in the United States and the public health impact of delaying disease onset," *Am J Public Health*, vol. 88, no. 9, pp. 1337-1342, 1998.

[3] G. Waldemar, B. Dubois, M. Emre, J. Georges, I. G. McKeith, M. Rossor, P. Scheltens, P. Tariska, and B. Winblad, "Recommendations for the diagnosis and management of Alzheimer's disease and other disorders associated with dementia: EFNS guideline," *European Journal of Neurology*, vol. 14, no. 1, pp. 1-26, 2007.

[4] G. Bartzokis, "Alzheimer's Disease as Homeostatic Responses to Age-related Myelin Breakdown," *Neurobiol of Aging*, vol. 32, no. 8, pp. 1341-1371, 2011.

[5] G. Bartzokis, P. H. Lu, and J. Mintz, "Quantifying Age-Related Myelin Breakdown with MRI: Novel Therapeutic Targets for Preventing Cognitive Decline and Alzheimer's Disease," *Journal of Alzheimer's Disease*, vol. 6, no. 6, pp. 53-59, 2004.

[6] George Bartzokis, P. H. Lu, and Jim Mintz, "Human Brain Myelination and Beta-amyloid Deposition in Alzheimer's Disease," *Alzheimer's & Dementia*, vol. 3, no. 2, pp. 122-125, 2007.

[7] P. D. Meek, E. K. McKeithan, and G. T. Schumock, "Economic considerations in Alzheimer's disease," *Pharmacotherapy*, vol. 18, no. 2, pp. 68-73, 1998.

[8] Ron Brookmeyer, Elizabeth Johnson, Kathryn Ziegler-Graham, and H. Michael Arrighi, "Forecasting the Global Burden of Alzheimer's Disease," *Alzheimer's & Dementia*, vol. 3, no. 3, pp. 186-191, 2007.

[9] Y. S. Kim, B. S. Soh, and S.-G. Lee, "A new wearable input device: SCURRY," *IEEE Trans. Industrial Electronics*, vol. 52, no. 6, pp. 1490-1499, 2005.

[10] Y. S. Suh, "Attitude estimation by multiple-mode Kalman filters," *IEEE Trans. Industrial Electronics*, vol. 53, no. 4, pp. 1386-1389, 2006.

[11] F. J. Berenguer and F. M. Monasterio-Huelin, "Zappa, a quasi-passive biped walking robot with a tail- modeling, behavior, and kinematic estimation using accelerometers," *IEEE Trans. Industrial Electronics*, vol. 55, no. 9, pp. 3281-3289, 2008.
[12] S.-H. P. Won, F.Golnaraghi, and W. W. Melek, "A fastening tool tracking system using an IMU and a position sensor with Kalman filters and a fuzzy expert system," *IEEE Trans. Industrial Electronics*, vol. 56, no. 5, pp. 1782-1792, 2009.
[13] J. S. Wang, Y. L. Hsu, and J. N. Liu, "An inertial-measurement-unit-based pen with a trajectory reconstruction algorithm and its applications," *IEEE Trans. Industrial Electronics*, vol. 57, no. 10, pp. 3508-3521, 2010.
[14] J. S. Wang and F. C. Chuang, "An accelerometer-based digital pen with a trajectory recognition algorithm for handwritten digit and gesture recognition," *IEEE Trans. Industrial Electronics*, vol. 59, no. 7, pp. 2998-3007, 2012.
[15] N. K. Nadkarni, E. Mawji, W. E. McIlroy, and S. E. Black, "Spatial and temporal gait parameters in Alzheimer's disease and aging," *Gait & Posture*, vol. 30, no. 4, pp. 452-454, 2009.
[16] T. Nakamura, K. Meguro, and H. Sasaki, "Relationship between falls and stride length variability in senile dementia of the Alzheimer type," *Gerontology*, vol. 42, no. 2, pp. 108-113, 1996.
[17] K. E. Webster, J. R. Merory, and J. E. Wittwer, "Gait variability in community dwelling adults with Alzheimer disease," *Alzheimer Disease and Associated Disorders*, vol. 20, no. 1, pp. 37-40, 2006.
[18] S. Gillain, E. Warzee, F. Lekeu, V. Wojtasik, D. Maquet, J.-L. Croisier, E. Salmon, and J. Petermans, "The value of instrumental gait analysis in elderly healthy, MCI or Alzheimer's disease subjects and a comparison with other clinical tests used in single and dual-task conditions," *Annals of Physical and Rehabilitation Medicine*, vol. 52, no. 6, pp. 453-474, 2009.